(11) Cosgrove, T. *Macromolecules* **1982**, *15*, 1290.
(12) Klein, J.; Pincus, P. *Macromolecules* **1982**, *15*, 1129.
(13) Croxton, C. *J. Phys. A* **1983**, *16*, 4343.
(14) Ben-Shaul, A.; Szleifer, I.; Gelbart, W. M. *J. Chem. Phys.* **1985**, *83*, 3597.
(15) Scheutjens, J. M. H. M.; Fleer, G. J. *Macromolecules* **1985**, *18*, 1882.
(16) Cosgrove, T.; Heath, T.; van Lent, B.; Leermakers, F.; Scheutjens, J. *Macromolecules* **1987**, *20*, 1692.
(17) Cosgrove, T.; Cohen Stuart, M. A.; Vincent, B. *Adv. Colloid Interface Sci.* **1986**, *24*, 143.
(18) Helfand, E.; Wasserman, Z. R. *Macromolecules* **1978**, *11*, 960.
(19) Noolandi, J.; Hong, K. M. *Macromolecules* **1982**, *15*, 482.
(20) Gerber, P. R.; Moore, M. A. *Macromolecules* **1977**, *20*, 476.
(21) Semenov, A. N. *Sov. Phys.-JETP (Engl. Transl.)* **1985**, *61*, 733.
(22) Milner, S. T.; Witten, T. A.; Cates, M. E., preprint.
(23) Takahashi, A.; Kawaguchi, M. *Adv. Polym. Sci.* **1982**, *46*, 1.
(24) Israelachvili, J. N.; Adams, G. E. *Nature (London)* **1976**, *262*, 774.
(25) Israelachvili, J. N.; Adams, G. E. *J. Chem. Soc., Faraday Trans. 1* **1978**, *74*, 975.
(26) Klein, J. *Nature (London)* **1980**, *288*, 248.
(27) Klein, J. *J. Chem. Soc., Faraday Trans. 1* **1983**, *79*, 99.
(28) Israelachvili, J. N.; Tirrell, M.; Klein, J.; Almog, Y. *Macromolecules* **1984**, *17*, 204.
(29) Klein, J.; Luckham, P. F. *Macromolecules* **1984**, *17*, 1041.
(30) Almog, Y.; Klein, J. *J. Colloid Interface Sci.* **1985**, *106*, 33.
(31) Hadziioannou, G.; Patel, S.; Granick, S.; Tirrell, M. *J. Am. Chem. Soc.* **1986**, *108*, 2869.
(32) Taunton, H. J.; Toprakcioglu, C.; Fetters, L. J.; Klein, J. *Nature (London)* **1988**, *332*, 712.
(33) Yamakawa, H. *Modern Theory of Polymer Solutions*; Harper and Row: New York, 1971.
(34) Edwards, S. F. *Proc. Phys. Soc., London* **1965**, *93*, 605.
(35) Ho, J.-S.; Muthukumar, M., submitted for publication in *Macromolecules*.
(36) Cosgrove, T.; Heeth, T. G.; Ryan, K.; Crowley, T. L. *Macromolecules* **1987**, *20*, 2879.

Dielectric Dispersion of Narrow-Distribution Poly(hexyl isocyanate) in Dilute Solution

Sanaye Takada, Takashi Itou, Hideaki Chikiri, Yoshiyuki Einaga, and Akio Teramoto*

Department of Macromolecular Science, Osaka University, Toyonaka, Osaka, 560 Japan.
Received May 25, 1988; Revised Manuscript Received July 20, 1988

ABSTRACT: Dielectric dispersion measurements were made on dilute solutions of narrow-distribution poly(hexyl isocyanate) in toluene to obtain the mean-square dipole moment $\langle\mu^2\rangle$ and dielectric relaxation time τ_D as functions of molecular weight and temperature. Analysis of the data for $\langle\mu^2\rangle$ at 25 °C in terms of the wormlike chain model of Kratky and Porod yielded a value of 27 700 for qM_L, with q and M_L being the persistence length and molar mass per unit contour length of the polymer, respectively. The data for τ_D at 25 °C as a function of molecular weight were accurately described by the equation for τ_D of Yoshizaki and Yamakawa for wormlike cylinders, and the result of the analysis was combined with the above qM_L value to give M_L = 740 nm^{-1}, q = 37 nm, and d = 1.5 nm, with d being the diameter of the cylinder. These parameter values were in good agreement with those estimated previously from viscosity data. The τ_D data at 10 and 40 °C were also represented by the same equation with the parameter values determined from viscosity data at the respective temperatures, thus establishing the validity of the Yoshizaki–Yamakawa theory of τ_D. The measured dielectric dispersions corrected for the sample's polydispersity in molecular weight were still polydisperse with respect to relaxation time, and the polydispersity increase with increasing molecular weight was more remarkable than predicted by the Yoshizaki–Yamakawa theory.

From various solution properties,[1-8] polyisocyanates of the general repeating unit –NRCO– are shown to be semiflexible; that is, they belong to those polymers classified between rodlike polymers and flexible polymers. Their conformational characteristics such as the mean-square radius of gyration etc. are well described by the wormlike chain model of Kratky and Porod.[1,4,6-8] Due to large cumulative dipole moments along their backbone chains, they exhibit dilute solution dielectric dispersions depending remarkably on molecular weight.[1-4,9,10] It is also noted that the reported dielectric dispersions in dilute solution cannot be described by the dispersion of the Debye type; in other words, they are usually polydisperse in relaxation time.[1,2,9,10] The reason for this polydispersity, among others, may be the sample's polydispersity in molecular weight and the presence of internal motional modes. In this connection, Yoshizaki and Yamakawa[11] have recently developed a theory of dielectric dispersion of helical wormlike chains in dilute solution, which gives an expression of the dielectric relaxation time τ_D and predicts a dielectric dispersion polydisperse with respect to relaxation time. They have treated the wormlike chain of Kratky and Porod as a special case of helical wormlike chains.

In the present study, we measured the dielectric constant and loss of dilute solutions of poly(hexyl isocyante) (PHIC) in toluene using narrow-distribution samples covering a range of molecular weight between 4410 and 910000. We have chosen this polymer because, in addition to the fact that it has been studied extensively with respect to the wormlike chain nature,[1,4,6-8] it is shown to have varying stiffness depending on the solvent conditions employed.[5-8,12] Thus the purpose of the present study is to provide dielectric dispersion data for PHIC free from molecular weight polydispersity and information about the polydispersity in dielectric relaxation time, thus enabling one to examine the quantitative validity of the theoretical predictions.

Experimental Section

Poly(hexyl isocyanate) samples were synthesized by polymerizing hexyl isocyanate in a toluene–dimethylformamide mixture with NaCN dispersed in dimethylformamide as an initiator.[13,14] Thirteen samples thus synthesized weighing about 130 g were separated into a number of fractions and 16 middle fractions were chosen for the present study. Their molecular weights and molecular weight distributions were determined by light scattering, sedimentation equilibrium, and gel permeation chromatography (GPC) as described elsewhere.[8] The numerical results are sum-

0024-9297/89/2222-0973$01.50/0 © 1989 American Chemical Society

Table I
Molecular Weights of PHIC Samples Studied[a]

sample	$10^{-4}M_w$	$(M_z/M_w)_{SED}$	$(M_z/M_w)_{GPC}$
W-70	0.441	1.4	
W-6	0.79[b]		
W-5	1.1_4	1.15	
W-4	1.31,[a] 1.29[b]		1.05
W-3	1.56,[a] 1.52[b]		1.05
Z-2	2.09	1.06	1.06
J2-2	3.2,[a,b] 3.08[c]		1.11
L-2	4.07	1.06	1.05
S2-2	6.1,[a] 5.9[b]		1.08_6
K-2	6.8, 6.64[c]	1.02	1.06
MO-2	9.8,[a] 10.2[b]		1.08
NRX-12	13.3, 12.2[c]	1.05	1.06
RX-2	16.2[a,b]		1.07
Z-20	24.4	1.05	1.07
H-14	51		
H-12	91		

[a] M_v from $[\eta]$ in 1-chlorobutane at 25 °C. [b] M_v from $[\eta]$ in toluene at 25 °C. [c] M_n; SED, sedimentation equilibrium.

Table II
Wormlike Chain Parameters of Poly(hexyl isocyanate)

solvent	temp, °C	M_L, nm^{-1}	q, nm	d, nm	method[b]
hexane[6]	25	715	42	1.6	LS + VIS
1-chlorobutane[7]	25	760	35	1.5	VIS
toluene[8]	10	730	41	1.6[a]	VIS
	25	740	37	1.6	VIS
	40	750	34	1.6[a]	VIS
DCM[8]	20	740	21	1.6[a]	VIS
toluene	25	740	37	1.5	DIEL

[a] Assumed value. [b] LS = light scattering; VIS = viscosity; DIEL = dielectric dispersion (this work).

marized in Table I, where M_z and M_w refer to the z-average and weight-average molecular weights, respectively. The molecular weights of some of the samples were determined only by viscometry using the $[\eta]$–M_w relationship in toluene of 25 °C and/or osmometry, i.e., they are the viscosity-average molecular weight M_v or number-average molecular weight M_n. It can be seen from the values of M_z/M_w given in this table that all these samples except samples W-70 and W-5 are close to monodisperse. Therefore, in the analysis to follow, we will not differentiate M_v from M_w and simply let $M_v = M_w = M$. It was found[8] that the GPC curves for these samples were almost symmetric and their molecular weight distribution curves were closely approximated by the distribution functions of the logarithmic normal type characterized by the M_z/M_w values given in this table. Table II gives the reported wormlike chain parameters of PHIC under various solvent conditions.[6-8]

The standard techniques for measuring complex dielectric constants in the radiofrequency range were followed by a transformer bridge described before.[15] A twin-T type bridge (Fujisoku DLB1101D) was used to supplement data at frequencies higher than 1 MHz. The measurements were made for both solutions and the solvent toluene at 10, 25, and 40 °C.

Results

Dielectric Dispersion Curves. Figure 1 shows plots of $\Delta\epsilon'/c$ and $\Delta\epsilon''/c$ versus logarithms of frequency f for a dilute solution of sample K-2 in toluene of 25 °C, where $\Delta\epsilon'$ and $\Delta\epsilon''$ are the differences in dielectric constant and dielectric loss between the solution and the solvent toluene, respectively, and c is the mass concentration of the polymer. Both $\Delta\epsilon'/c$ and $\Delta\epsilon''/c$ show substantially single dispersions centered around 18 kHz, and $\Delta\epsilon'/c$ approaches a constant value at low frequencies but vanishes at high frequencies.

Figure 2 shows a plot of $\Delta\epsilon''/c$ versus $\Delta\epsilon'/c$, i.e., the Cole–Cole plot constructed from the data in Figure 1. The static dielectric increment $\Delta\epsilon = \epsilon_s - \epsilon_\infty$ was evaluated from the height of the $\Delta\epsilon'/c$ curve at low frequencies or more

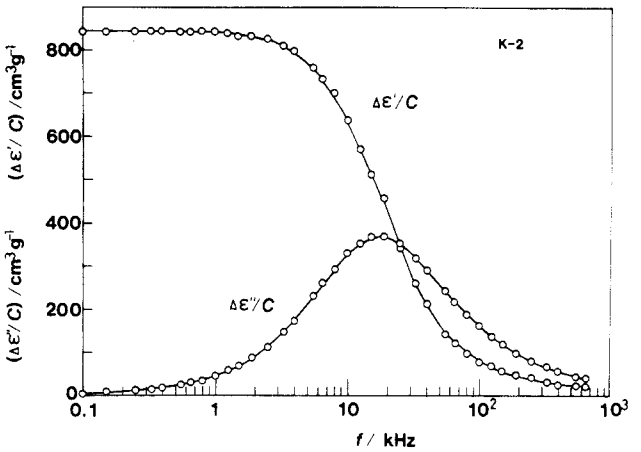

Figure 1. Plots of $\Delta\epsilon'/c$ and $\Delta\epsilon''/c$ versus f for sample K-2 in toluene at 25 °C. $c = 8.72 \times 10^{-4}$ g cm^{-3}.

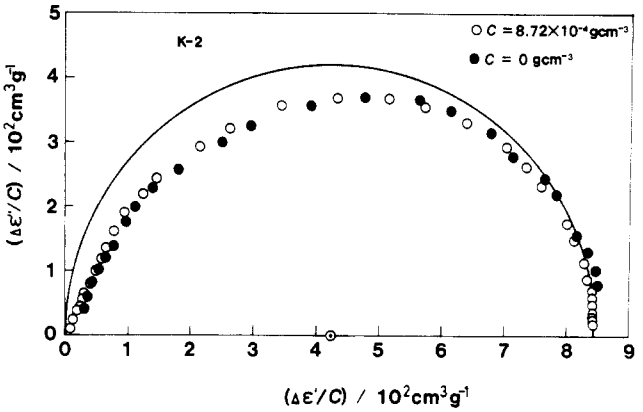

Figure 2. Cole–Cole plot for sample K-2 in toluene at 25 °C constructed from the data in Figure 1.

precisely from the segment cut on the abscissa by the Cole–Cole plot as shown in Figure 2; ϵ_s and ϵ_∞ are the static dielectric constant and the dielectric constant at the limit of higher frequencies of the solution, respectively. Since we are dealing with dilute solutions, $\Delta\epsilon$ is a small fraction of ϵ_∞, which is usually close to the solvent dielectric constant ϵ_0. The critical frequency f_c, which is related to the dielectric relaxation time τ_D by $\tau_D = 1/(2\pi f_c)$, is obtained as the frequency at which the dielectric loss curve or the Cole–Cole plot exhibits a maximum; $f_c = 17.7$ kHz.

In Figure 2, the open circles represent the experimental data in Figure 1, while the solid semicircle represent the Debye dispersion corresponding to the $\Delta\epsilon/c$ value as determined above. It can be seen that the data points appear somewhat below the Debye curve; the observed loss curve is broader than the corresponding Debye curve, with a lower peak height. Thus this polymer shows a dielectric dispersion polydisperse in relaxation time. As will be discussed below, however, the deviation from monodispersity is much less than the reported data,[1-3] which had been taken for polymer samples broader in molecular weight distribution.

Figure 3 illustrates how $\Delta\epsilon'/c$ and $\Delta\epsilon''/c$ at fixed frequencies change with c. While $\Delta\epsilon'/c$ decreases linearly with c at each frequency, $\Delta\epsilon''/c$ decreases, stays nearly constant, or increases with c, depending on the frequency examined. The infinite-dilution value for either quantity can be obtained by extrapolation to $c = 0$ with reasonable accuracy. However, it is noted that since the data refer to relatively low concentrations, there is no large difference in either quantity between the extrapolated value and that at the lowest concentration. Indeed, the filled circles in Figure 2 represent the extrapolated values, which are al-

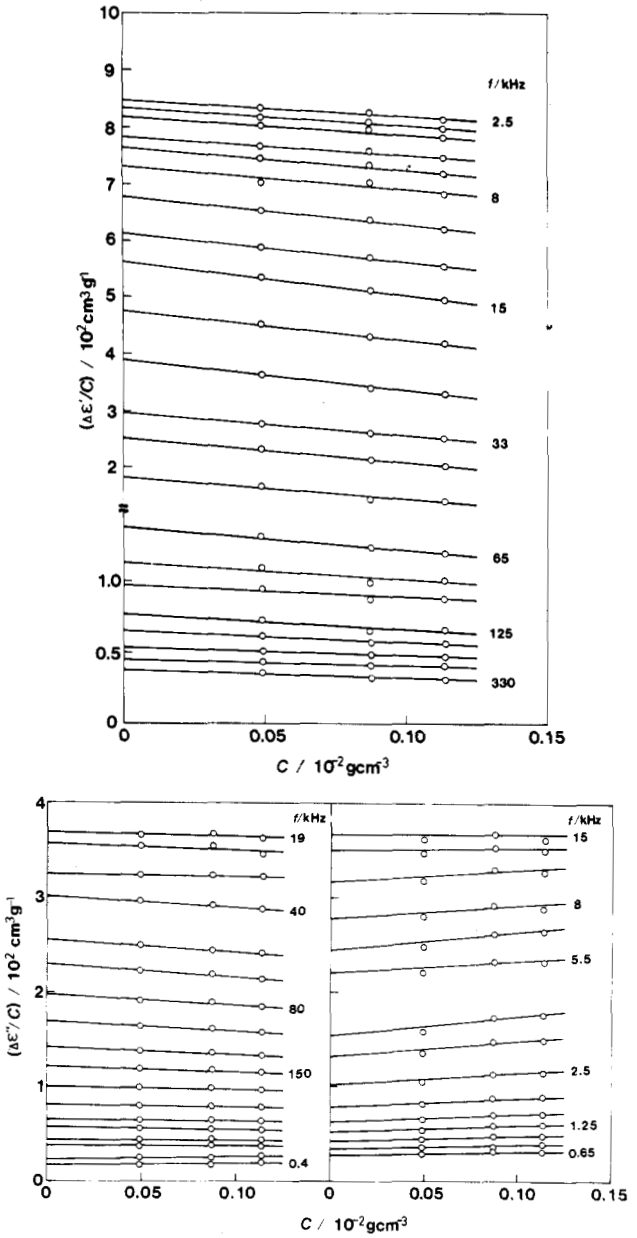

Figure 3. Concentration dependence of dielectric increments at the indicated f for sample K-2 in toluene at 25 °C. (Top) Plots of $\Delta\epsilon'/c$ versus c; (bottom) plots of $\Delta\epsilon''/c$ versus c.

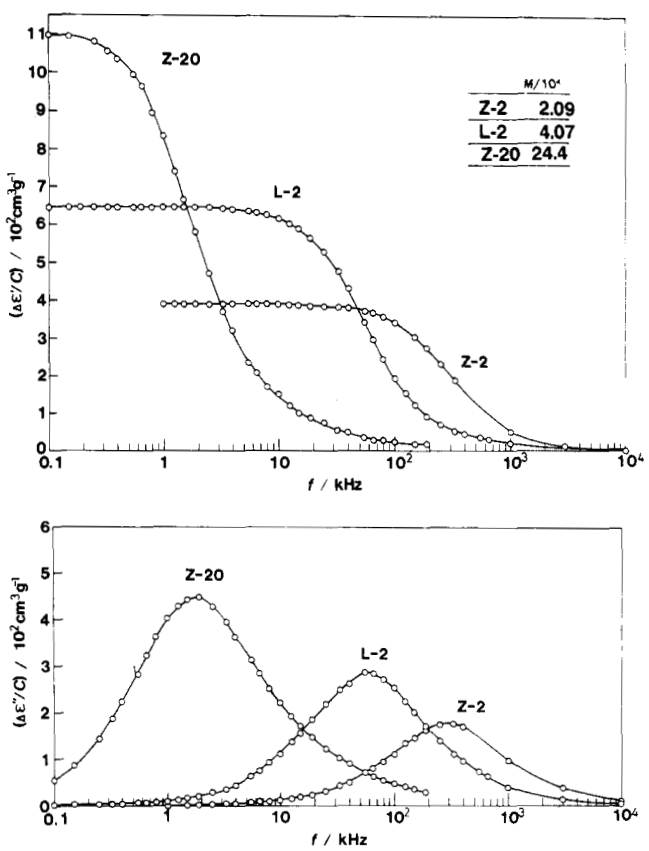

Figure 4. (Top) Plots of $\Delta\epsilon'/c$ versus f for PHIC fractions in toluene at 25 °C. (Bottom) Plots of $\Delta\epsilon''/c$ versus f for PHIC fractions in toluene at 25 °C.

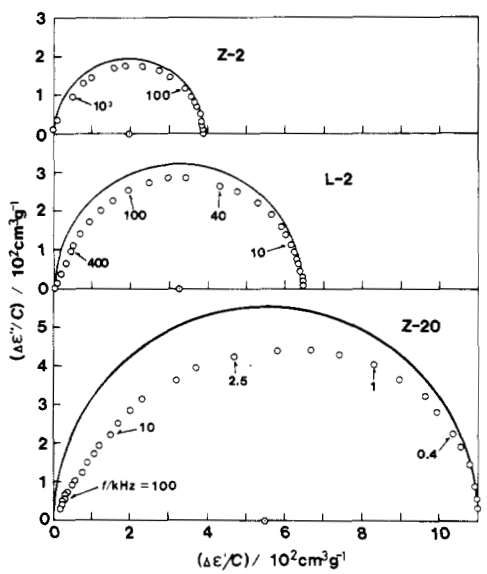

Figure 5. Cole–Cole plots for PHIC fractions in toluene at 25 °C. Circles, experimental data; solid semicircles, Debye curves.

most indistinguishable from those obtained at a finite concentration of 8.72×10^{-4} g cm^{-3}. Therefore, in what follows, all the data taken at such low concentrations are regarded as the infinite-dilution values except those for the three samples of the highest molecular weights, for which both $\Delta\epsilon/c$ and f_c were extrapolated to infinite dilution.

Figure 4 shows dielectric dispersion curves for three PHIC samples having different molecular weights in toluene at 25 °C. In part a, for each sample $\Delta\epsilon'/c$ approaches a constant value at low frequencies, which increases remarkably with increasing molecular weight, but it eventually vanishes at higher frequencies through a dispersion region. Panel b illustrates how the dielectric loss curve changes with the molecular weight of the sample. The loss curve for each sample has a single peak, whose height appears to parallel the plateau height of $\Delta\epsilon'/c$.

Figure 5 presents these data in the form of a Cole–Cole plot. It is noted that the data points (open circles) follow nearly the Debye curve (solid semicircle) for sample Z-2, the lowest molecular weight sample among the three, whereas they appear significantly below the corresponding Debye curve for the higher molecular weight samples.

Specific Dielectric Increment and Dielectric Relaxation Time. Similar data were obtained for the other samples in toluene at 25 °C and for some samples in toluene at 10 and 40 °C. Values of the specific dielectric increment $\Delta\epsilon/c$ and of the critical frequency f_c evaluated from such data are summarized in Table III.

Figure 6 shows $\Delta\epsilon/c$ in toluene at 25 °C as a function of molecular weight M on a double-logarithmic plot. It can be seen that the plot starts with a slope of about unity characteristic of rodlike dipoles at low M and tends to level

Table III
Dielectric Dispersion Data for PHIC in Toluene

sample	f_c, kHz	$\Delta\epsilon/c$, 10^2 cm^3 g^{-1}	$\langle\mu^2\rangle^{1/2}$, 10^2 D
	25 °C		
W-70		0.90	0.806
W-6		1.61	1.44
W-5	1300	2.29	2.06
W-4	900	2.60	2.34
W-3	630	3.04	2.75
Z-2	295	3.88	3.64
J2-2	88	5.60	5.49
L-2	55	6.47	6.56
S2-2	25	7.77	8.65
K-2	17.7	8.43	9.68
MO-2	8.4	9.43	12.5
NRX-12	5.5	10.2	14.9
RX-2	3.8	10.4	16.6
Z-20	1.8	11.0	20.9
H-14	0.55	12.1	31.8
H-12	0.197	12.2	42.1
	10 °C		
W-5	1000	2.35	2.04
Z-2	210	4.41	3.78
Z-20	1.25	12.5	21.7_4
H-14	0.360	13.4	32.6
	40 °C		
W-5		2.08	2.02
Z-2	360	3.68	3.63
L-2	78	5.81	6.36
Z-20	2.70	9.17	19.6
H-14	0.76	9.30	28.5_2

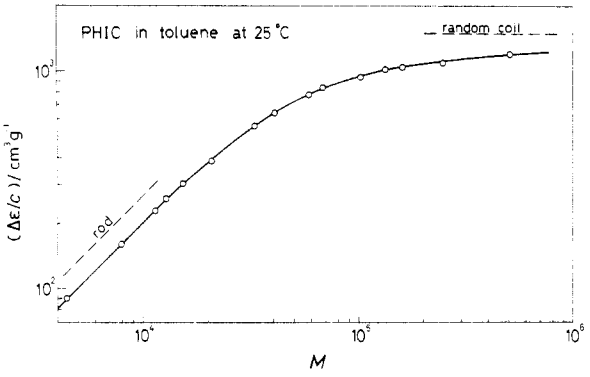

Figure 6. Double-logarithmic plot of $\Delta\epsilon/c$ versus M for PHIC in toluene at 25 °C.

off to a constant value for higher M, exhibiting a feature of random coil polymers with a type A dipole, namely, linear polymers with finite dipole moments along the chain contour.[16] Values of the dielectric relaxation time τ_D in toluene at 25 °C are plotted double logarithmically against M in Figure 7. As shown about with $\Delta\epsilon/c$, τ_D also displays a transition from the rodlike behavior to the random-coil behavior as the molecular weight is increased.

Discussion

Evaluation of the Mean-Square Dipole Moment. The "vacuum" dipole moment $\langle\mu^2\rangle^{1/2}$ directly associated with the conformation of the polymer in solution can be evaluated from $\Delta\epsilon/c$ and M by correcting for the effect of the surrounding medium. So far the following three equations have been used for this evaluation. They can be expressed as

$$\langle\mu^2\rangle = \frac{3k_BT(\Delta\epsilon/c)M}{4\pi N_A}P \qquad (1)$$

where k_B is the Boltzmann constant, T the absolute temperature, and N_A the Avogadro constant. Wada[17] neglected the medium effect and simply put $P = 1$. On the other hand, Bur and Roberts[2] derived on the basis of the Onsager spherical cavity model an expression for P

$$P = 9/(\epsilon_s + 2)(\epsilon_0 + 2) \qquad (2)$$

Applequist and Mahr[18] used Buckingham's theory derived for ellipsoidal dipoles,[19] which gives P as a complicated function of ϵ_s and ϵ_0 reflecting the molecular geometry. It can be shown that as ϵ_0 increases indefinitely, P approaches $^3/_2$ in the Buckingham equation but vanishes in the Bur–Roberts equation. The applicability of these equations may be checked by using solvents of different dielectric constants ϵ_0.

The conformation of PHIC depends on solvent conditions through the difference in chain stiffness until it reaches the rod limit at small enough molecular weights. Indeed, it has been shown that $[\eta]$–M plots for PHIC under different solvent conditions appear to merge into a single curve at low molecular weights.[8] Thus it is expected that $\langle\mu^2\rangle$ for a low molecular weight PHIC sample evaluated from $\Delta\epsilon/c$ may be independent of solvent polarity provided that an appropriate correction is applied. To test this expectation, dielectric measurements were made on sample W-4 (M = 13000) in toluene at 25 °C (ϵ_0 = 2.379), in chlorobenzene at 25 °C (ϵ_0 = 5.621), and in dichloromethane at 20 °C (ϵ_0 = 9.08). Table IV presents the values of $\langle\mu^2\rangle^{1/2}$ relative to that in toluene calculated from $\Delta\epsilon/c$ by the above three equations. Precisely speaking, a PHIC chain is more flexible in dichloromethane than in toluene,[5,8,12] and when corrected for this difference in flexibility

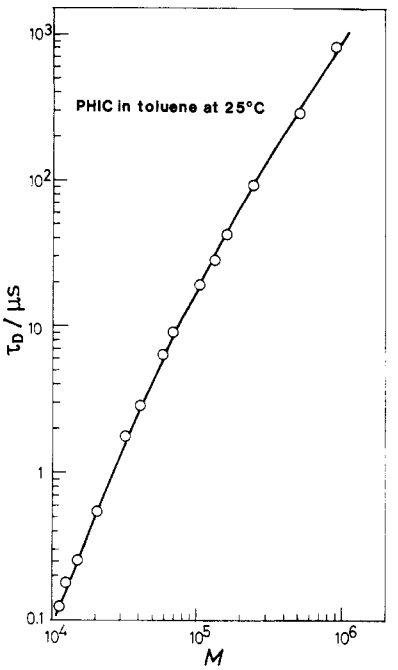

Figure 7. Double-logarithmic plot of dielectric relaxation time τ_D versus molecular weight M for PHIC in toluene at 25 °C.

Table IV
Vacuum Dipole Moments of Sample W-4 in Various Solvents Calculated According to the Indicated Equations

solvent	temp, °C	dipole moment[a] Bur–Roberts	Wada	Buckingham
toluene	25	1	1	1
chlorobenzene	25	0.481	0.844	0.943
DCM	20	0.341 (0.360)	0.862 (0.909)	0.994 (1.05)

[a] Relative to that in toluene. Values in parentheses are calculated for finite stiffness (see text).

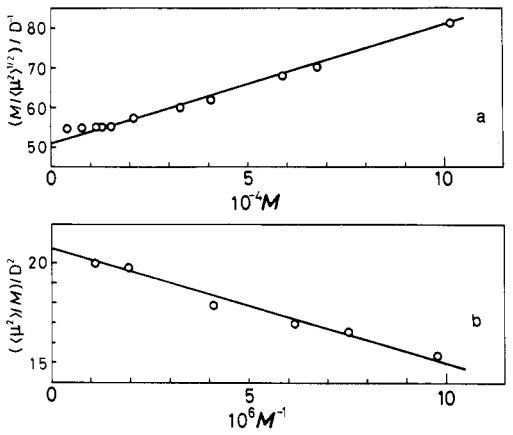

Figure 8. (a) Plot of $M/\langle\mu^2\rangle^{1/2}$ versus M and (b) plot of $\langle\mu^2\rangle/M$ versus M^{-1} for PHIC in toluene at 25 °C. See eq 4 and 5.

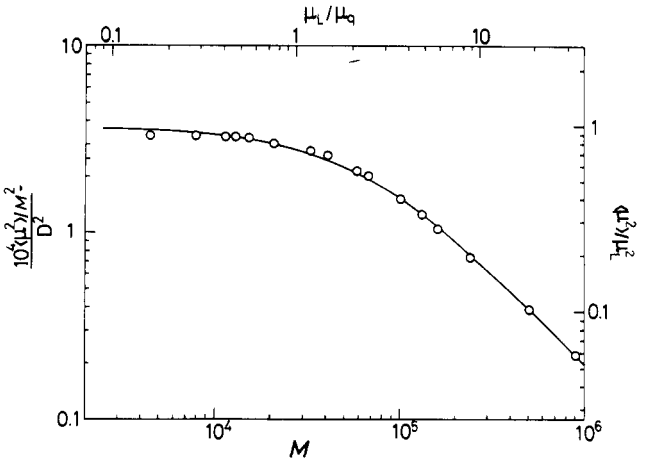

Figure 9. Molecular weight dependence of $\langle\mu^2\rangle/M^2$ for PHIC in toluene at 25 °C. Circles, experimental data; solid curve, theoretical values calculated according to eq 3 with M_L = 740 nm^{-1}, q = 37 nm, and μ_0 = 2.46 D (see text).

in a manner described below, the expected value of the dipole moment in dichloromethane is calculated to be 0.948 instead of unity. The values in parentheses have been estimated on this basis.

It can be seen in Table IV that eq 2 is inadequate because it gives different dipole moment values for the different solvents, whereas Buckingham's equation gives essentially the same values for the three solvents, in agreement with the above expectation. However, this equation is derived for rigid ellipsoids, and there is no guarantee for its applicability to higher molecular weight PHIC, where the molecular conformation is far from being a rigid ellipsoid. Wada's equation is simplest and gives dipole moment values not much removed from unity. Actually it gives dipole moment values substantially the same as those estimated by Buckingham's equation. Therefore we will use the values obtained by this equation in the analysis to follow. They are given on the fourth column in Table III.

Analysis in Terms of the Wormlike Chain Model. The mean-square dipole moment $\langle\mu^2\rangle$ for a Kratky–Porod chain with a cumulative dipole moment μ_L along the chain contour is expressed as[1]

$$\langle\mu^2\rangle/\mu_L^2 = 2/x - 2(1/x)^2(1 - e^{-x}) \quad (3)$$

where $x = \mu_L/\mu_q = L/q$ and L and q are the contour length and persistence length of the chain, respectively; $L = M/M_L$, with M_L being the molar mass per unit contour length.

It can be shown that this equation is well approximated by the following asymptotic expressions:

$$\langle\mu^2\rangle/M = 2(\mu_0/M_0)^2qM_L(1 - qM_L/M) \quad (qM_L/M \ll 1) \quad (4)$$

$$M/\langle\mu^2\rangle^{1/2} = (M_0/\mu_0)[1 + M/(6qM_L)] \quad (qM_L/M \gg 1) \quad (5)$$

where M_0 is the molar mass of monomeric unit and $\mu_0 = \mu_L/(M/M_0)$.

The lower panel of Figure 8 shows a plot of $\langle\mu^2\rangle/M$ versus M^{-1} with the data for relatively large M. As predicted by eq 4, the data points are fitted accurately by the straight line indicated, whose ordinate intercept and slope yield the result μ_0 = 2.46 D and qM_L = 27 700. It can be seen in the upper panel that $M/\langle\mu^2\rangle^{1/2}$ versus M obeys the linear relation predicted by eq 5 with these parameter values. Figure 9 shows a double-logarithmic plot of $\langle\mu^2\rangle/\mu_L^2$ versus L/q, where the data points (circles) follow closely the theoretical curve calculated by eq 3 with the above values for μ_0 and qM_L. It should be noted, however, that neither of the above equations allows separate estimate of q and M_L.

Recently Yoshizaki and Yamakawa[11] have derived a theoretical equation of τ_D for a wormlike cylinder on the basis of the helical wormlike chain model, which is the cylinder of a uniform diameter d whose contour is L long and follows the wormlike chain statistics. It is expressed as a function of L, q, and d by

$$\tau_D = \tau_{D,rod}Q(L/2q) \quad (6)$$

with

$$Q(x) = x^{-3}[x + (e^{-x} - 1)/2]^{3/2}[1 + 0.539\,526 \ln (1 + x)] \quad (7)$$

where $\tau_{D,rod}$ is the dielectric relaxation time of the straight cylinder of the same length and diameter given by

$$\tau_{D,rod} = \pi\eta_0L^3F_r(L/d)/6k_BT$$

with

$$F_r(x)^{-1} = \ln x + 2 \ln 2 - 11/6 - 8.25644[\ln (1 + x)]^{-1} + 13.0447x^{-1/4} - 62.6084x^{-1/2} + 174.0921x^{-3/4} - 218.8356x^{-1} + 140.2699x^{-5/4} - 33.2708x^{-3/2}$$

The data for τ_D in toluene of 25 °C were analyzed by eq 6 with various values assumed for d. It was found that particular sets of q and M_L gave good agreement between experiment and theory for a given value of d. However, it was impossible to determine all three parameters separately only from the τ_D data. Therefore we have combined this analysis with the above estimate of qM_L, with the result d = 1.5 nm, q = 37 nm, and M_L = 740 nm^{-1} in toluene at 25 °C. The solid curve in Figure 10 represents the theoretical value for $2k_BT\tau_D/\pi\eta_0d^3$ calculated for these parameters, which fits the experimental data accurately over the entire range of molecular weight investigated; η_0 is the solvent viscosity. As seen in Table II, these parameter values are in excellent agreement with those estimated previously from viscosity data.[8]

Equation 6 predicts that $\tau_D/\tau_{D,rod}$ be a unique function $Q(L/2q)$ of $L/2q$. Figure 11 shows a test of this prediction with all the τ_D data in toluene at the three temperatures investigated; the above values of d, M_L, and q at 25 °C and those at 10 and 40 °C determined from viscosity data are used. It can be seen that all the data points irrespective of molecular weight and temperature now form a single composite curve which is accurately represented by eq 6.

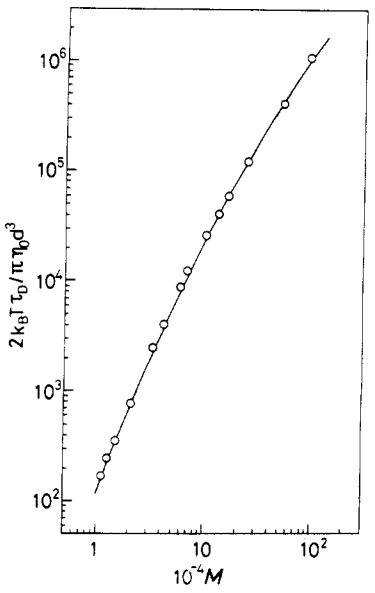

Figure 10. Molecular weight dependence of dielectric relaxation time. Circles, experimental data for PHIC in toluene at 25 °C; solid curve, the Yoshizaki–Yamakawa equation with M_L = 740 nm^{-1}, q = 37 nm, and d = 1.5 nm.

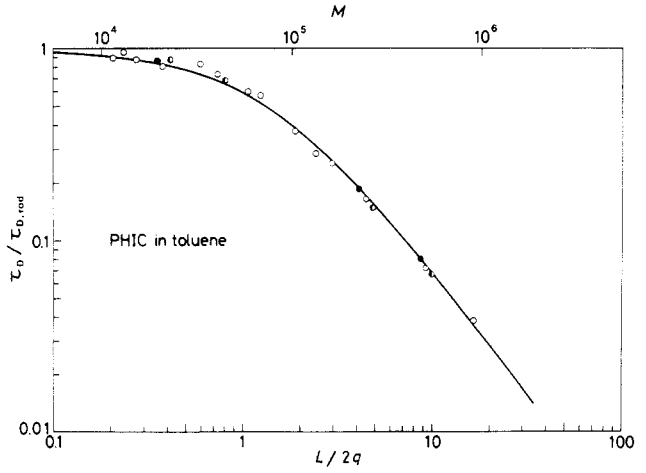

Figure 11. Double-logarithmic plot of $\tau_D/\tau_{D,rod}$ versus $L/2q$. Data for PHIC in toluene at 10 °C (●), 25 °C (○), and 40 °C (◐); solid curve, theoretical values according to eq 6 (see text).

Thus we conclude that the present dielectric dispersion data have well confirmed the wormlike chain nature of PHIC in dilute solution deduced from other data and established the validity of the Yoshizaki–Yamakawa theory of τ_D.

Polydispersity in Relaxation Time. As shown in Figures 2 and 5, the measured dielectric dispersion curves deviate more or less from those of the Debye type. The deviation can be conveniently measured by the half-width $W/2$ of the loss curve in logarithms of frequency ratio[1-3] and the peak height ξ of the loss curve relative to $^1/_2\Delta\epsilon/c$. For the Debye curve, $W/2$ = 1.144 and ξ = 1. The values of $W/2$ and ξ for the samples measured in toluene of 25 °C are given in Table V. It will be observed that in terms of $W/2$ and ξ, the deviation is not significant at low molecular weights but gets more remarkably with increasing M. It is noted, however, that the measured values of $W/2$ are considerably smaller than those reported by Bur and Roberts[2] for poly(butyl isocyanate), which are at least larger than 1.6. We may suggest the following causes for the deviation: the sample's polydispersity in molecular weight[1-3] and multiple modes of motion of the polymer chain.[11]

Table V
Deviation from the Debye Dispersion of the Dielectric Loss Curves for PHIC in Toluene at 25 °C[a]

sample	$W/2$	ξ	sample	$W/2$	ξ
H12	1.5	0.71	S2-2	1.30	0.85_7
H14	1.4_4	0.81	L-2	1.24	0.88_8
Z-20	1.38	0.81_7	J2-2	1.37	0.85_1
RX-2	1.37	0.81_3	Z-2	1.1_7	0.91_6
NRX-12	1.25	0.87_2	W-3	1.1_8	0.92_1[b]
MO-2	1.32	0.85_2	W-4	1.12	0.93_8[b]
K-2	1.26	0.87_8			

[a] $W/2$ = 1.144 and ξ = 1 for the Debye dispersion. [b] Determined from Cole–Cole plots.

Let us begin with examining how the observed dielectric dispersion is affected by the molecular weight polydispersity. The experimentally measured complex dielectric increment $\Delta\epsilon^*(f)$ may be expressed in terms of the distribution function $g(M)$ of molecular weight M as[3]

$$\Delta\epsilon^*(f) = \int_0^\infty (\Delta\epsilon' + i\Delta\epsilon'')g(M)\,dM \tag{8}$$

where $\Delta\epsilon'$ and $\Delta\epsilon''$ are the real and imaginary parts of the dielectric increment for species with molecular weight M. In the case where each molecular species has only one relaxation mechanism characterized by the relaxation strength $\Delta\epsilon(M)$ and relaxation time $\tau(M)$, $\Delta\epsilon'(f)$ and $\Delta\epsilon''(f)$ are given respectively by

$$\Delta\epsilon'(f) = \int_0^\infty \frac{\Delta\epsilon(M)}{1 + [2\pi f\tau(M)]^2}g(M)\,dM \tag{9}$$

$$\Delta\epsilon''(f) = \int_0^\infty \frac{2\pi f\tau(M)\Delta\epsilon(M)}{1 + [2\pi f\tau(M)]^2}g(M)\,dM \tag{10}$$

On the basis of the GPC data given elsewhere,[8] we assume that $g(M)$ is represented by a distribution function of the logarithmic normal type. Further we express $\Delta\epsilon(M)$ and $\tau(M)$ as

$$\Delta\epsilon(M) = \Delta\epsilon(M_w)(M/M_w)^\alpha \tag{11}$$

$$\tau(M) = \tau(M_w)(M/M_w)^\beta \tag{12}$$

where $\Delta\epsilon(M_w)$ and $\tau(M_w)$ are the corresponding values at molecular weight M_w and α and β are defined by

$$\alpha = \mathrm{d}[\ln \Delta\epsilon(M)]/\mathrm{d}[\ln M] \tag{13}$$

$$\beta = \mathrm{d}[\ln \tau(M)]/\mathrm{d}[\ln M] \tag{14}$$

In the analysis to follow, we assume that α and β are treated as constants depending on M_w and use those values that would be obtained empirically from the experimental data given in Figures 6 and 7, respectively. This assumption may be justified because the integral in eq 8 is carried out in a relatively narrow range of M for our samples.

Values for $\Delta\epsilon'(f)$ and $\Delta\epsilon''(f)$ of a given sample were calculated by eq 9 and 10 so that the values for M_z/M_w, $\Delta\epsilon/c$, and τ_D would be consistent with their experimental values. Typical results from such calculations are illustrated in Figure 12, where the calculated Cole–Cole plots of four samples (solid curves) are compared with the corresponding Debye curves (dashed curves). It can be seen that for the three lower molecular weight samples, the data points are fitted accurately by the calculated curves, indicating that the small deviation from the Debye curve is ascribed only to the sample's polydispersity in molecular weight. However, for sample Z-20, the solid curve is rather close to the Debye curve but deviates far

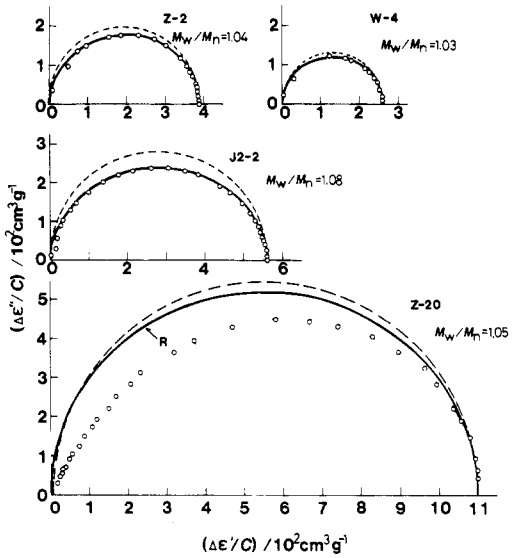

Figure 12. Cole–Cole plots for PHIC fractions in toluene at 25 °C. Circles, experimental data; dashed semicircles, Debye curves; thick solid curves, theoretical curves calculated by eq 9 and 10 for the indicated values of M_w/M_n (see text).

above the data points. This shows that the dispersion is still polydisperse in relaxation time even after being corrected for the sample's polydispersity. The polydispersity was found to set in at M_w of about 70 000 and become remarkable with increasing molecular weight. Yoshizaki and Yamakawa[11] have predicted a deviation which originates from internal modes of motion of the chain, but it is considerably smaller than that observed here. This invites a further theoretical investigation of this problem.

Acknowledgment. We thank Dr. Takashi Norisuye for stimulating discussions. This work was in part supported by the Institute for Macromolecular Research, Osaka University.

Registry No. PHIC, 26746-07-6.

References and Notes

(1) Bur, A. J.; Fetters, L. J. *Chem. Rev.* **1977**, *76*, 727.
(2) Bur, A. J.; Roberts, D. E. *J. Chem. Phys.* **1969**, *51*, 406.
(3) Bur, A. J. *J. Chem. Phys.* **1970**, *52*, 3813.
(4) Fetters, L. J.; Yu, H. *Macromolecules* **1971**, *4*, 385.
(5) Berger, M. N.; Tidswell, B. M. *J. Polym. Sci., Polym. Symp.* **1973**, *42*, 1063.
(6) Murakami, H.; Norisuye, T.; Fujita, H. *Macromolecules* **1980**, *13*, 345.
(7) Kuwata, H.; Murakami, H.; Norisuye, T.; Fujita, H. *Macromolecules* **1984**, *17*, 2731.
(8) Itou, T.; Chikiri, H.; Teramoto, A. *Polym. J.* **1988**, *20*, 143.
(9) Lochhead, R. Y.; North, A. M. *Trans. Faraday Soc.* **1972**, *68*, 1089.
(10) Anderson, J. S.; Vaughan, W. E. *Macromolecules* **1975**, *8*, 454.
(11) Yoshizaki, T.; Yamakawa, H. *J. Chem. Phys.* **1984**, *81*, 982.
(12) Conio, G.; Bianchi, E.; Ciferri, A.; Krigbaum, W. R. *Macromolecules* **1984**, *17*, 2731.
(13) Shashoua, V. E.; Sweeny, W.; Tietz, R. F. *J. Am. Chem. Soc.* **1960**, *82*, 866.
(14) Aharoni, S. M. *Macromolecules* **1979**, *12*, 94.
(15) Matsumoto, T.; Nishioka, N.; Teramoto, A.; Fujita, H. *Macromolecules* **1974**, *7*, 824.
(16) Stockmayer, W. H. *Pure Appl. Chem.* **1967**, *15*, 539.
(17) Wada, A. J. *Chem. Phys.* **1959**, *31*, 495; *Bull. Chem. Soc. Jpn.* **1960**, *33*, 822.
(18) Applequist, J.; Mahr, T. G. *J. Am. Chem. Soc.* **1966**, *88*, 5419.
(19) Buckingham, A. D. *Aust. J. Chem.* **1952**, *6*, 93, 323.

Excluded-Volume Effects in Rubber Elasticity. 4. Nonhydrostatic Contribution to Stress

J. Gao and J. H. Weiner*

Department of Physics and Division of Engineering, Brown University, Providence, Rhode Island 02912. *Received May 11, 1988*

ABSTRACT: Molecular dynamics simulations of idealized network models demonstrate that the noncovalent excluded-volume (EV) interaction makes a significant nonhydrostatic contribution to the stress tensor when ϕ, the fraction of occupied volume, is above ~0.3. This contribution grows with ϕ and, at the same time, the covalent contribution decreases. As a result, the noncovalent EV interaction rapidly becomes the dominant source of deviatoric stress in the network. The simulations show that the covalent bonds introduce directional screening of the noncovalent EV interaction; this provides the mechanism with its nonhydrostatic contribution. They also show that the average force in the covalent bonds decreases with increase in ϕ; this is the reason for the decrease in the covalent contribution.

1. Introduction

We continue in this paper our investigations into the role of excluded volume (EV) in rubber elasticity. As in the previous papers of this series,[1-3] our principal tool is the computer simulation of idealized atomic systems. Our hope is that the study of these systems may provide insight into the details of the mechanisms of atomic interactions, both covalent and noncovalent; the resulting physical picture can then be compared with those underlying the various molecular theories that have been but forward for rubberlike solids.

We have begun our studies with highly idealized systems for two reasons. The first is the practical one, that computer time requirements go up rapidly with increased realism of the model. This makes difficult extensive studies, including the effects of wide parameter variation. The second reason for starting with simple models is that it is easier to grasp the essential features of what is going on when they are employed. When the significant features of the behavior of the idealized models become clear, we plan to use them as a guide for the study of more realistic models and to determine to what extent the observations on the idealized models carry over.

Of principal concern in these studies has been the nature of the contribution of the noncovalent EV interaction to the stress. In our previous work, where the simulations were restricted to systems with relatively small occupied volume fractions, we found that the EV contribution to

0024-9297/89/2222-0979$01.50/0 © 1989 American Chemical Society